iScience, Volume *27*

Supplemental information

Structure basis for recognition of plant Rpn10 by phytoplasma SAP05 in ubiquitin-independent protein degradation

Liying Zhang, Yunxiang Du, Qian Qu, and Qingyun Zheng

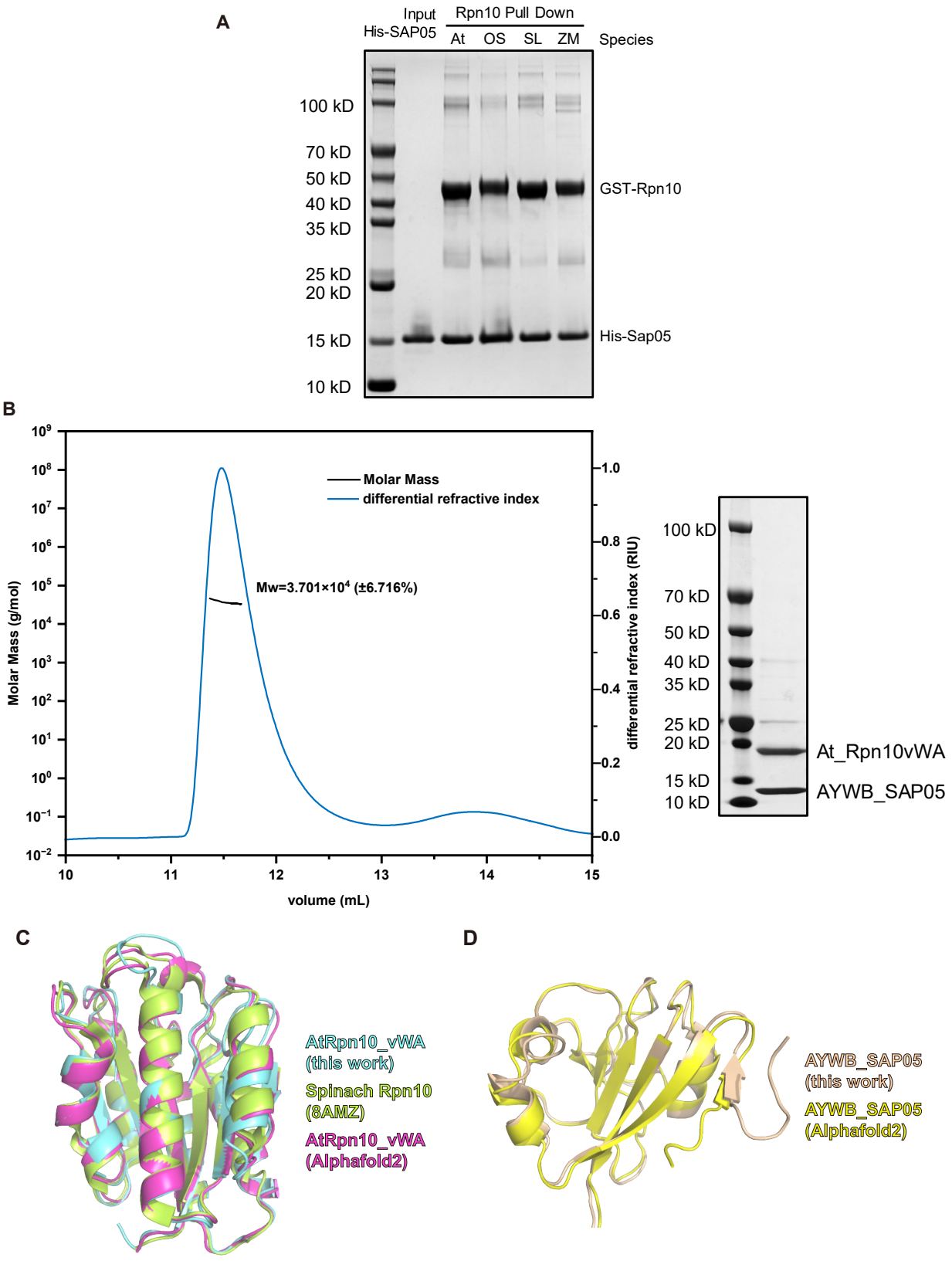

Figure S1. Crystallization and subunit structure of AYWB_SAP05-AtRpn10 complex, related to Figure 1 and STAR Methods. A) Pull down assay of His6-AYWB-SAP05 with GST-Rpn10 from different plant species. B) AYWB_SAP05 and AtRpn10_vWA formed a stable 1:1 heterodimeric complex in size exclusion chromatography coupled with multiangle light scattering (SEC-MALS) analysis, which was analyzed by SDS-PAGE. C) Structural alignment of AtRpn10 (cyan) to hRpn10 (in 8AMZ, lime) and Alphafold2 predicted model (magenta). D) Structural alignment of AYWB_SAP05 (wheat) to Alphafold2 predicted model (yellow).

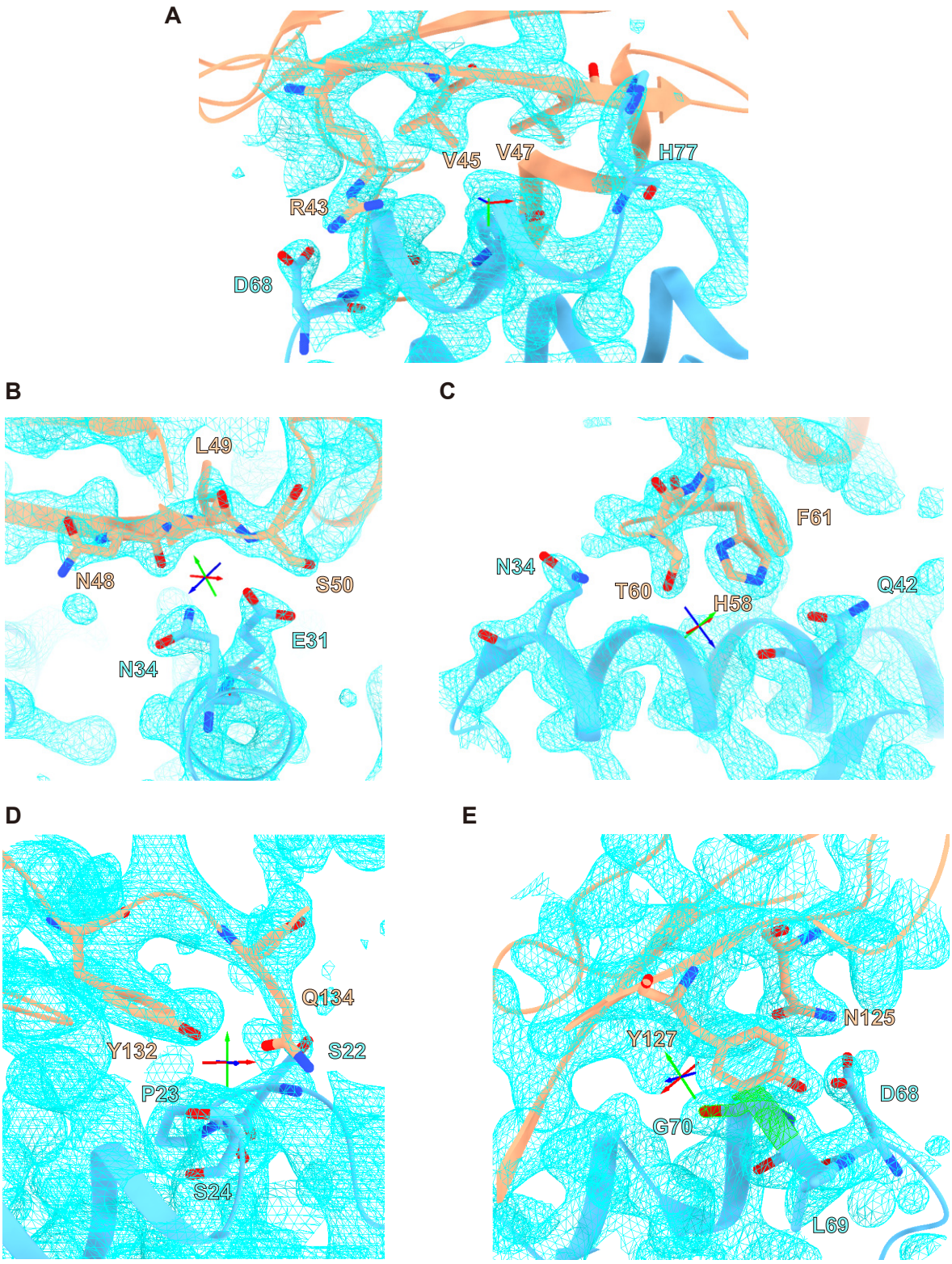

Figure S2. Detailed interaction information in AYWB_SAP05-AtRpn10 complex, related to Figure 2. The residues involved in the interactions are shown in sticks, the 2mFo-DFc crystallographic map from the .mtz file is indicated by cyan mesh. AtRpn10 is in indigo and AYWB_SAP05 is in wheat. A) B) C) Detailed structure of β-side, α-side, and vertex interface on V-shape peptide. D) E) Detailed structure of two anchors of C-ter peptide.

A

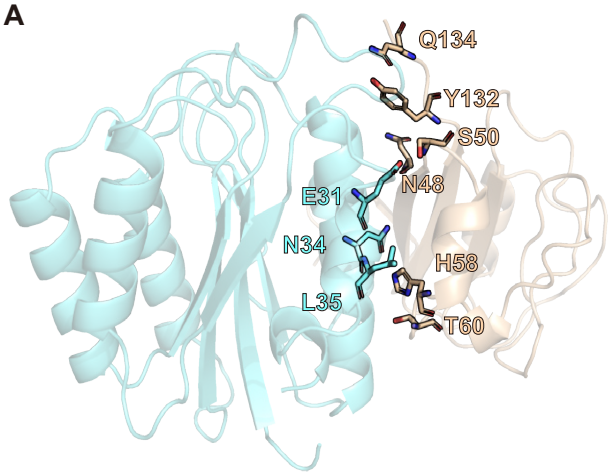

B

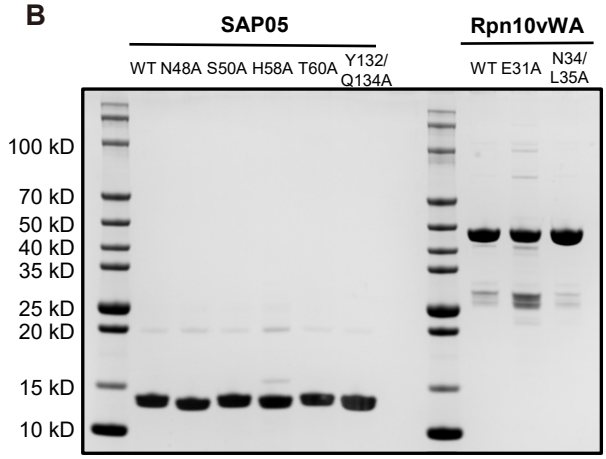

C

	K_D / μM	SE / μM	pK_D (-log K_D)
AYWB_SAP05 variant binding to immobilized wild type AtRpn10			
WT	6.38	0.26	5.195
N48A	6.24	0.46	5.205
T60A	10.1	1.1	4.995
Y132Q134A	43.6	2.1	4.360
S50A	209	36	3.679
H58A	Undetectable	Undetectable	Undetectable
AtRpn10 variant binding to immobilized wild type AYWB_SAP05			
WT	0.400	0.039	6.398
N34L35A	24.6	3.3	4.609
E31A	Undetectable	Undetectable	Undetectable

D

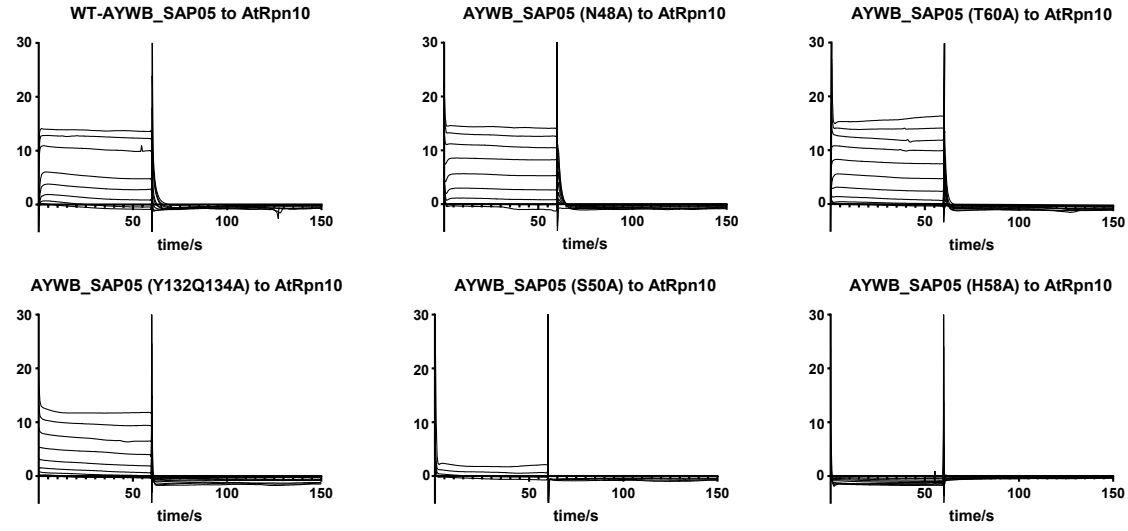

E

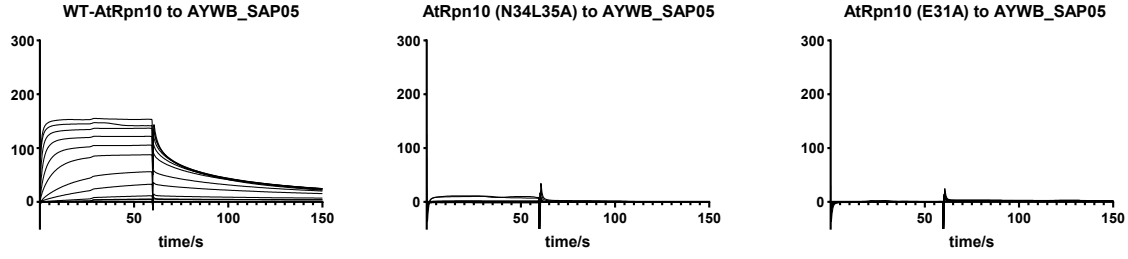

Figure S3. Mutations of key interface residues of AYWB_SAP05 or AtRpn10, related to Figure 3. A) The locations of mutated key residues of AYWB_SAP05 and AtRpn10 in the complex structure. B) SDS-PAGE analysis of wild type (WT) protein and each SAP05, Rpn10 mutants, which are the inputs of SPR assay. C) Table of dissociation constant (KD) value, standard error (SE), and pKD of each variant in SPR assay. D) SPR raw sensorgram of each AYWB_SAP05 variant binding to AtRpn10. E) SPR raw sensorgram of each AtRpn10 variant

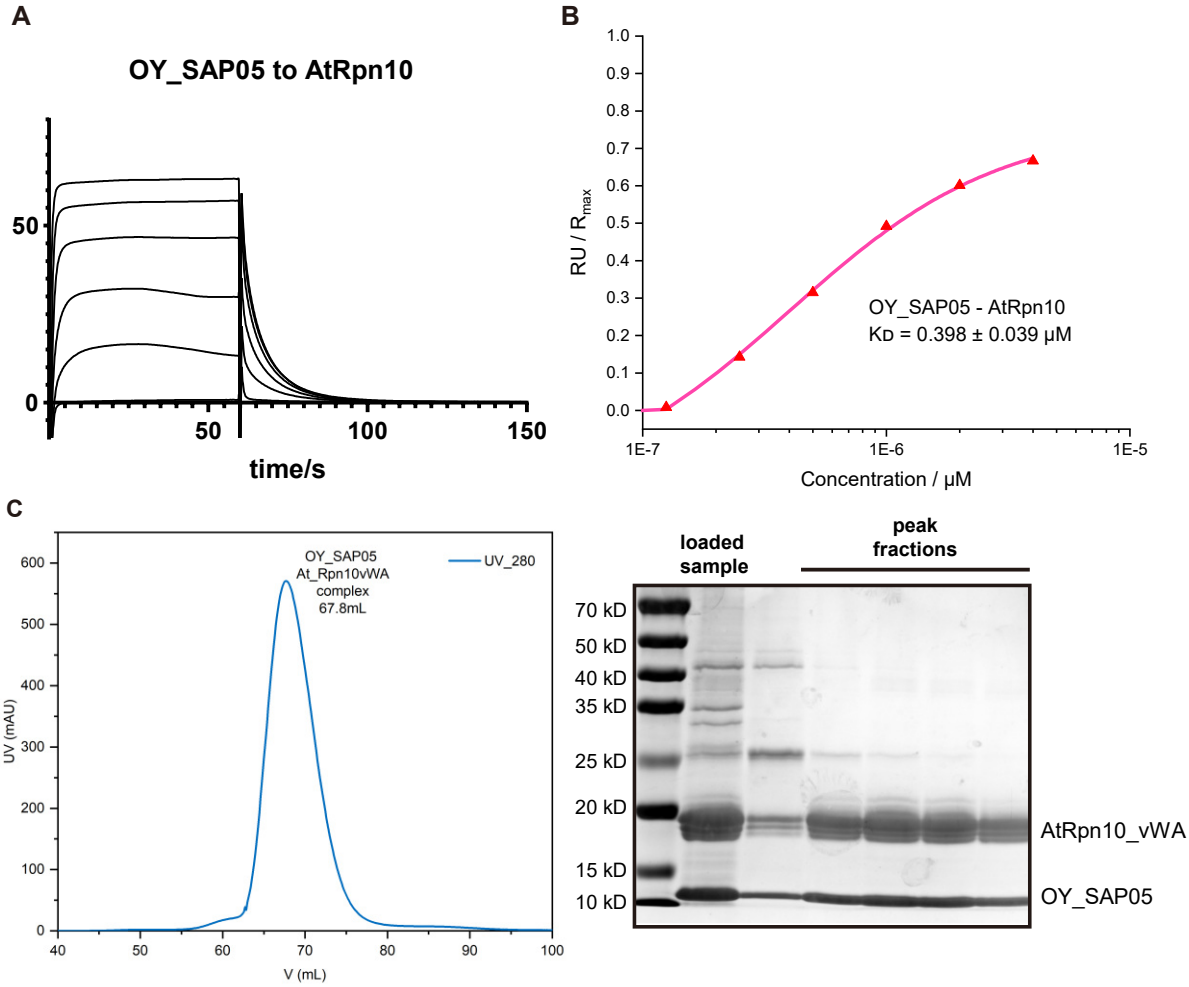

Figure S4. Reconstitution of OY_SAP05-AtRpn10 complex, related to Figure 4 and STAR Methods. A) SPR raw sensorgram of WT OY_SAP05 binding to AtRpn10. B) The curve of response value versus concentration of OY_SAP05 in the SPR binding assay of OY_SAP05 binding to immobilized AtRpn10. C) OY_SAP05 and AtRpn10_vWA formed a stable 1:1 heterodimeric complex in gel filtration, which was analyzed by SDS-PAGE.

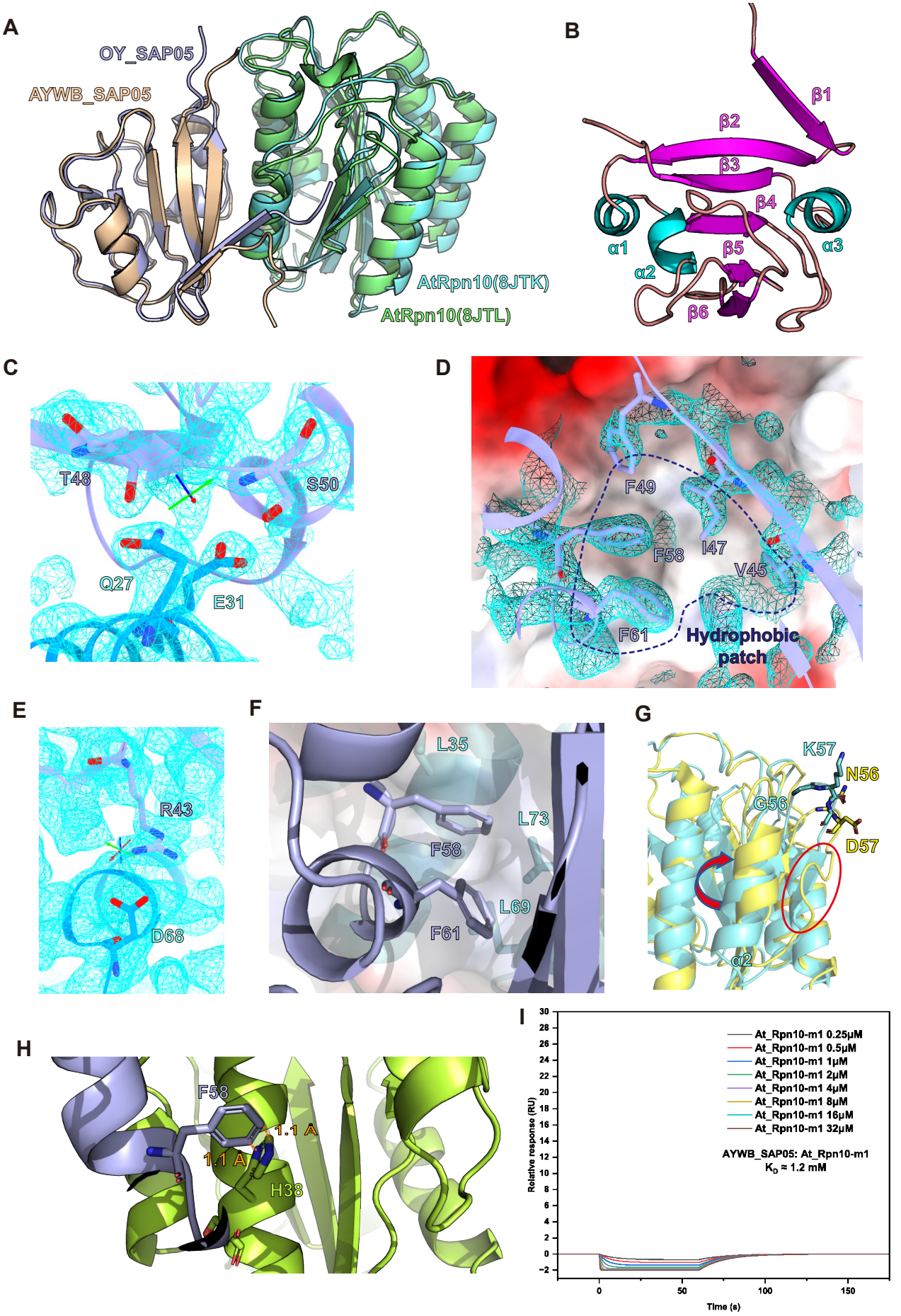
A
OY_SAP05
AYWB_SAP05
AtRpn10(8JTK)
AtRpn10(8JTL)
B
β1
β2
β3
β4
α1
β5
α3
α2
β6
C
T48
S50
Q27
E31
D
F49
F58
I47
V45
F61
Hydrophobic patch
E
R43
D68
F
L35
L73
F58
L69
F61
G
K57
N56
G56
D57
α2
H
F58
1.1 Å
1.1 Å
H38
I
At_Rpn10-m1 0.25μM
At_Rpn10-m1 0.5μM
At_Rpn10-m1 1μM
At_Rpn10-m1 2μM
At_Rpn10-m1 4μM
At_Rpn10-m1 8μM
At_Rpn10-m1 16μM
At_Rpn10-m1 32μM
AYWB_SAP05: At_Rpn10-m1
K_D ≈ 1.2 mM
Relative response (RU)
Time (s)

Figure S5. Detailed structure of OY_SAP05-AtRpn10 complex, related to Figure 4. A) Superposing the structure of the OY_SAP05-AtRpn10 complex (8JTL) to the AYWB_SAP05-AtRpn10 complex (8JTK). B) Secondary structures and their number in OY_SAP05. C) Detailed structure of hydrogen bonds formed at the vertex of OY_SAP05 V-shape peptide. D) Residues interact with the hydrophobic patch on the AtRpn10 surface. E) New hydrogen bond formed between R43 of OY_SAP05 and D68 of AtRpn10. F) F58 associated with F61 mediate stable hydrophobic interaction with AtRpn10 and thus cover the contribution of hydrogen bond formed by H58 of AYWB_SAP05. G) Alignment of our crystal structure to the human Rpn10 (PSMD4 in PDB 6MSB) vWA domain structure. The key mutations were shown in sticks and the conformation differences were pointed out with the red circle and arrow. H) Docking the structures of hRpn10 to OY_SAP05 with reference to AtRpn10_vWA-OY_SAP05 complex, there is a clash between H38 of hsRpn10 and F58 of OY_SAP05. I) SPR binding assay between GST-AtRpn10_38GA39 > HS (m1) mutant and AYWB_SAP05.

A

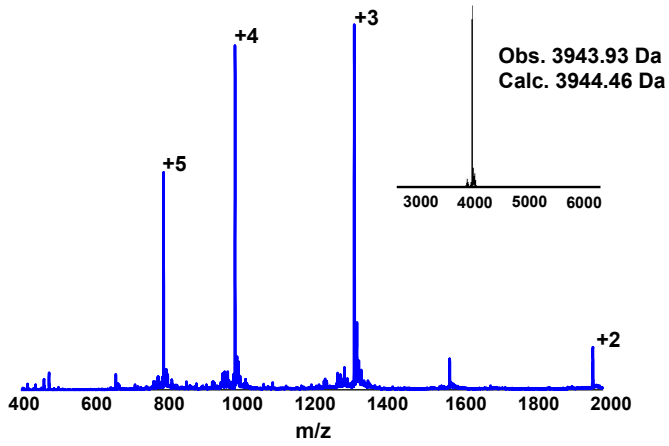

Peptide sequence:
RIVNVNLSNIDILKKHETF-GSGS-NMYIFWQYEQ

B

	K_D / μM	SE / μM	pK_D (-log K_D)
OY_SAP05 variant binding to immobilized wild type AtRpn10			
WT	0.398	0.039	6.400
R43A	2.31	0.46	5.636
T48S50A	2.77	0.70	5.558
F58A	34.0	7.9	4.469
F61A	49.4	3.7	4.306
V45R	61.2	8.3	4.213
Q59P60A	89.1	7.2	4.050

Figure S6. AYWB_SAP05 derived peptide and OY_SAP05 variants binding to AtRpn10, related to Figure 4. A) The Sequence and ESI-MS spectrum of our V-shape-C-ter peptide. B) Table of dissociation constant (KD) value, standard error (SE), and pKD of each OY_SAP05 variant in SPR assay.